HHS Public Access

Author manuscript

J Drug Deliv Sci Technol. Author manuscript; available in PMC 2020 August 01.

Published in final edited form as:

J Drug Deliv Sci Technol. 2019 August ; 52: 165–176. doi:10.1016/j.jddst.2019.04.029.

Processability of AquaSolve™ LG polymer by hot-melt extrusion: Effects of pressurized CO_2 on physicomechanical properties and API stability

Mashan Almutairi[a], **Bjad Almutairy**[a], **Sandeep Sarabu**[a], **Ahmed Almotairy**[a], **Eman Ashour**[a], **Suresh Bandari**[a], **Amol Batra**[b], **Divya Tewari**[b], **T. Durig**[b], **Michael A. Repka**[a,c,*]

[a]Department of Pharmaceutics and Drug Delivery, University of Mississippi, University, MS 38677, USA

[b]Ashland Specialty Ingredients, Wilmington, DE 19808, USA

[c]Pii Center for Pharmaceutical Technology, University of Mississippi, University, MS 38677, USA

Abstract

The objective of this study was to investigate the processability of AquaSolve™ hydroxypropyl methylcellulose acetate succinate L grade (HPMCAS LG) via hot-melt extrusion and to examine the effect of pressurized carbon dioxide (P-CO_2) on the physicomechanical properties of efavirenz (EFA)-loaded extrudates. To optimize the process parameters and formulations, various physical mixtures of EFA (30%, 40%, and 50%, w/w) and HPMCAS LG (70%, 60%, and 50%, w/w), respectively, were extruded using a co-rotating twin-screw extruder with a standard screw configuration, with P-CO_2 injected into zone 8 of the extruder. Thermal characterization of the extrudates was performed using differential scanning calorimetry and thermogravimetric analysis. Scanning electron microscopy was employed to study the morphology and porosity of the formulations. Notably, the macroscopic morphology changed to a foam-like structure by P-CO_2 injection resulting in an increased specific surface area, porosity, and dissolution rate. Thus, HPMCAS LG extrusion, coupled with P-CO_2 injection, yielded faster dissolving extrudates. Stability studies indicated that HPMCAS LG was able to physically and chemically stabilize the amorphous state of high-dose EFA. Furthermore, the milling efficiency of the extrudates produced with P-CO_2 injection improved because of their increased porosity.

Graphical Abstract

*Corresponding author. Department of Pharmaceutics and Drug Delivery & Pii Center for Pharmaceutical Technology, School of Pharmacy, University of Mississippi, University, MS 38677, USA, marepka@olemiss.edu (M. A. Repka).

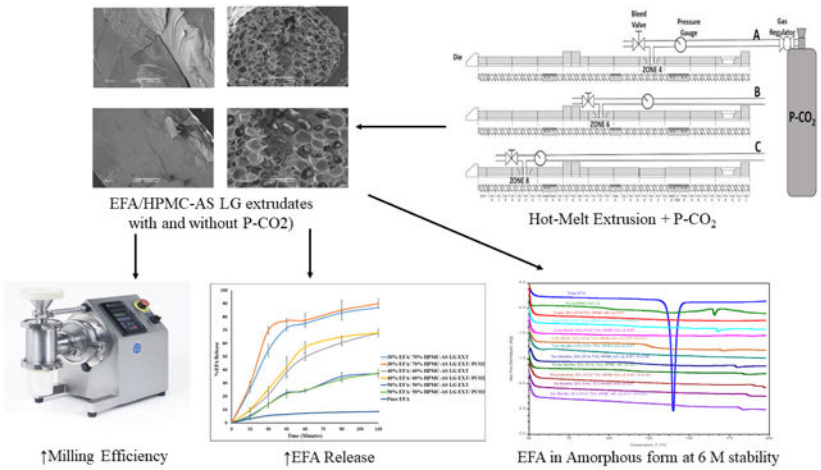

Keywords

Hot-melt extrusion; Pressurized carbon dioxide; HPMCAS LG; Milling efficiency; Porosity

1. Introduction

Over a period of more than two decades, hot-melt extrusion (HME) has evolved into one of the most promising pharmaceutical processing technologies [1]. HME has several advantages over conventional pharmaceutical processing technologies, such as a short processing time and the capacity for continuous processing, which does not require the use of water or potentially toxic organic solvents [2,3]. HME is generally used for the solubility enhancement of active pharmaceutical ingredients (APIs) [4] and is suitable for manufacturing various dosage forms, such as pellets, tablets, and transmucosal products, or for various applications, such as controlled release formulations, targeted drug delivery, and taste-masking formulations [5,6].

Recently, several HME products have been commercially approved and marketed, resulting in a further increase of interest in this technology in the pharmaceutical industry. However, many pharmaceutical polymeric systems experience thermal and/or viscoelastic challenges during HME, which cannot be ignored. One thermal challenge is material degradation during processing, and a viscoelastic challenge is the feasibility of extrusion. Moreover, APIs exhibit their own individual limitations, such as high melting temperatures (T_ms) and/or low degradation temperatures [7]. Physicochemical properties of APIs, including glass transition and melting point temperatures, degradation temperatures, and miscibility or solubility in a polymer carrier, have to be carefully considered since they have significant effects on HME processes as well as on the final product [8–11].

Polymeric carriers are usually the largest component in amorphous dispersion formulations. Thus, physicochemical properties of the polymer carrier, such as the molecular weight, viscosity, and glass transition temperature (T_g), can significantly influence HME processing conditions and the performance of the final drug products [12,13]. The degradation temperature and viscoelastic properties of polymers are major factors that must be

considered for the HME process [14]. Therefore, determination of thermal and viscoelastic properties of various drug/polymer mixtures helps identify the optimal HME processing parameters (extrusion temperature, screw speed, feeding rate, motor load, and screw design) and provide insights into the properties of the extrudate [15].

More than 50% of common pharmaceutical polymers used for HME cannot be processed without a processing aid because these polymers have viscosities exceeding the defined maximum viscosity limit within the HME processing window. Often, the added API can plasticize polymers, which reduces viscosity of the complex and leads to smooth extrusion. If API cannot adequately plasticize polymeric carriers, alternative formulation or processing strategies are necessary to utilize these carriers [7].

One such strategy is the addition of plasticizers [16]. Typically, plasticizers increase the free volume between polymer chains, causing decreases in the T_g and melt viscosity [17]. Normally, plasticizers are utilized at a concentration of 5–30% (w/w) by being physically mixed with a pre-extrusion blend [18–20]. Plasticizer addition, therefore, results in significantly larger dosage forms [16]. Plasticizers also remain mobile and can lead to further physical and chemical changes, as well as to instability of the final drug product. Therefore, it would be preferable to find an alternative to traditional plasticizers for pharmaceutical extrusion. Recently, supercritical carbon dioxide (sc-CO_2) and subcritical (pressurized) carbon dioxide (P-CO_2) have been investigated as temporary plasticizers [21,22]. However, it has been observed that sc-CO_2 and P-CO_2 act as foaming agents [23], which increase the surface area and porosity of polymers, resulting in enhanced dissolution [24].

Hydroxypropyl methylcellulose acetate succinate (HPMCAS) has been shown to be a very effective crystallization inhibitor in amorphous solid dispersions (ASDs) [25,26]. HPMCAS polymers have a T_g of 120 °C but regularly require extrusion temperatures in excess of 170 °C, even with plasticization used to reduce the high motor torque, due to high melt viscosity [27]. HPMCAS L grade (LG) has the highest concentration of succinoyl groups compared with that in other grades (MG and HG), which results in a higher hydrophilicity. Succinoyl groups also play an important role in stabilizing ASDs by inducing high-affinity binding to the hydrophobic drug surface, leading to crystal growth inhibition of an API [28]. However, it has been reported that the succinoyl group shows sensitivity to a high temperature (above 160 °C) during the extrusion process by producing a free acid, which corresponds to a decrease in the succinoyl content. Considering the above factors, HPMCAS LG was selected as a polymer to investigate the effects of physical and mechanical properties of physical mixtures of a model API and HPMCAS LG on drug solubility and stability. The suitability of the combination and a correlation between drug/polymer properties and the HME process were assessed in this study. In addition, the effect of carbon dioxide as a foaming agent and its impact on the physicomechanical properties and performance of the extrudates were investigated.

2. Materials and methods

2.1. Materials

AquaSolve™ HPMCAS LG and efavirenz (EFA) were donated by Ashland Specialty Ingredients (Wilmington, DE). Carbon dioxide (CO_2) was supplied in gas cylinders (pure clean) by Airgas (Tupelo, MS). All other chemicals and reagents used in the present study were of analytical grade and obtained from Fisher Scientific (Fair Lawn, NJ).

2.2. Methods

2.2.1. Thermogravimetric analysis—Thermogravimetric analysis (TGA) was performed for EFA and HPMCAS LG to determine the optimal processing temperatures for extrusion and stability studies using a Pyris 1 thermogravimetric analyzer with the Pyris manager software (PerkinElmer Life and Analytical Sciences, Shelton, CT). Approximately 5–7 mg of samples (API and polymer) was weighed in an aluminum pan and heated from 25 °C to 200 °C at 10 °C/min under a nitrogen atmosphere.

2.2.2. Hot-melt extrusion—A co-rotating twin-screw intermeshing extruder (16-mm Prism Euro Lab; Thermo Fisher Scientific, Waltham, MA) was used to perform HME. The extruder is divided into 10-barrel zones adjacent to the gravimetric feeder. The standard manufacturer's screw configuration was used for this study, which consists of four conveying zones and three mixing zones. P-CO_2 was injected into the extruder using a high-pressure regulator connected to a flexible stainless-steel hose with armor casing. The other end of the hose was connected to a four-way connection and fitted with a pressure gauge, bleed valve, and check valve (ball type for a unidirectional flow of gas), with the latter connected to an injection port at zone 8 (conveying zone) of the extruder (Fig. 1). The P-CO_2 flow rate was regulated using the regulator knob. Preliminary extrusion experiments were conducted to determine the processing temperature for the pure polymer over a temperature range of 140 to 190 °C at 75 and 100 rpm (Table 1). Based on these experiments, extrusion in the presence of P-CO_2 was studied at 190 °C. Formulations were extruded at a drug load of 20%, 30%, 40%, and 50%, with and without P-CO_2.

2.2.3. Preparation of physical mixtures—After optimizing the parameters of the HME process, various physical mixtures were prepared with the following composition: EFA (30, 40, and 50%, w/w) and HPMCAS LG (70, 60, and 50%, w/w), respectively. The mixtures were blended using a V-shell blender ((MaxiBlend™, GlobePharma, North Brunswick, NJ) at 25 rpm for 15 minutes. All the formulations listed in (Table 2) were successfully extruded at the selected processing conditions.

2.2.4. Milling efficiency analysis—Prior to the analysis, HME extrudates were milled using a laboratory-scale FitzMill (model L1A; Fitzpatrick, Perth Amboy, NJ), and the particle size distribution and milling efficiency were studied using a vibrating sieve shaker (Performer III SS-3; Gilson). The fraction below 600 μm was used for further investigation. To study the milling efficiency of formulations before and after P-CO_2 injection, 25 g of each melt-extruded sample was milled for 3 min at 3,000 rpm, and the particle size distribution was estimated using a vibrating sieve method. A set of sieves with known mesh

sizes (75, 125, 250, 420, 600, and 840 μm) and known tare weights were stacked on one another, and a known amount of the powder was placed in the top sieve. The whole stack was placed on a vibrating plate at an amplitude of 1.5 mm for 10 minutes, after which each sieve was weighed to obtain the average distribution of particle sizes.

2.2.5. Drug content analysis—Assay methods detailed in the United States Pharmacopeia (USP) were used. The EFA content in extrudates was determined by dissolving extrudates in a phosphate buffer solution (pH 6.8) and performing ultraviolet (UV) spectrophotometric analysis against a blank buffer solution. The analysis was performed using a UV spectrophotometer (Genesys 6; Thermo Fisher Scientific, Madison, WI) at a wavelength of 247 nm, at which absorbance of the polymer is negligible. The measured drug content was compared to the calculated value. The experimental value was an average of triplicate measurements.

2.2.6. Dissolution studies—*In vitro* dissolution testing was conducted on milled and #40-sieved extrudate samples to investigate the influence of P-CO_2 injection to the polymer matrix on drug release from HPMCAS LG extrudates. The results were compared with those obtained for pure crystalline EFA. A USP dissolution apparatus II (Hanson SR8; Hanson Research, Chatsworth, CA) was used with a paddle rotation speed of 50 rpm, and samples were incubated in pH 6.8 phosphate buffer at 37 ± 0.5 °C for 2 h. At predetermined time intervals, 2-mL aliquots were collected and replaced with an equal volume of a fresh dissolution medium. The aliquots withdrawn were filtered through a 10-μm filter, and EFA was measured by UV spectrophotometry (Genesys 6; Thermo Fisher Scientific, Madison, WI) at 247 nm. All dissolution tests were carried out in triplicate, and the mean ± standard deviation was determined.

2.2.7. Differential scanning calorimetry—The solid-state nature of pure EFA, pure HPMCAS LG, their physical mixtures, and the corresponding extrudates was assessed by differential scanning calorimetry (DSC) to determine the impact of P-CO_2 on thermal properties during formulation processing. The analysis was preformed using a differential scanning calorimeter (DSC 25 Discovery series; TA Instruments, New Castle, DE) coupled with a refrigerated cooling system. Samples of 4–8 mg were weighed using a Mettler Toledo scale and then placed in non-perforated aluminum pans, which were crimped before testing, with an empty crimped aluminum pan used as a reference cell. Calorimetry scans were carried out from 50 to 200 °C at a scanning rate of 10 °C/min. Volatiles were removed from the purging head with a nitrogen flow at 20 mL/min. Calibration of the instrument was performed using indium as the standard. After each scan completed, the melting points were analyzed, and the Trois® manager software was used for data analysis.

2.2.8. Powder X-ray diffraction measurements—The degree of crystallinity of pure EFA, pure HPMCAS LG, EFA in physical mixtures, and the respective extrudates was investigated using powder X-ray diffraction (XRD) with a Bruker D8 Focus X-ray diffractometer, operated at a voltage of 40 kV and a current of 40 mA. The powder was packed into a sample holder. Data for each sample were collected in a 2θ angle range of 4–

40° over 10 min in a continuous detector scan mode. A scanning step of 0.02° and a scanning step duration of 0.3 s were used.

2.2.9. Scanning electron microscopy (SEM)—Morphological characteristics and the degree of porosity of extrudates with different drug loads (30, 40, and 50%), with and without P-CO_2 treatment, were studied using a scanning electron microscope (JEOL JSM-5600) at a 25-, 50-, and 100-fold magnification and an accelerating voltage of 5 kV. Each specimen was fixed using a conductive, double-sided carbon adhesive tape and coated with gold using a Hummer® 6.2 sputtering system (Anatech, Ltd., Springfield, VA) in a high-vacuum evaporator prior to the test to avoid electrostatic charging.

2.2.10. Density and porosity estimation—True densities of milled extrudates for all formulations, as well as that of the pure polymer, were measured, with and without P-CO_2 injection, using an AccuPyc 1330 gas pycnometer S/N-4011 (Micromeritics Instrument Corp., Norcross, GA). Prior to each run, calibration was performed. The sample was filled in a 10-cm^3 sample cup, and the weight of the sample was recorded. The true density was measured at an equilibration rate of 0.0050 psig/min, and the number of purges was set to 10. Bulk and tapped densities were calculated by measuring the volume of 5 g of a milled extrudate in a 10-mL graduated cylinder. The porosity was calculated by using the following equation [29]:

$$\% \ Porosity = 1 - \frac{Bulk\ Density}{True\ Density} \times 100$$

2.2.11. Physical and chemical stability tests—Stability studies were conducted for 24 weeks by monitoring the crystalline content (using DSC), chemical stability (drug content estimation), *in vitro* dissolution, and physical appearance of samples. Extrudate samples were stored in 20-mL clear glass scintillation vials, which were sealed with screw caps, at 25 °C and 60% relative humidity. The samples were analyzed on the first day and after 1, 2, 3, and 6 months. Drug release profiles were obtained for samples removed from the stability chamber after 12 and 24 weeks.

3. Results and discussion

3.1. Hot-melt extrusion

Physicochemical properties of an API and polymeric carrier need to be considered carefully since they have a significant impact on the HME process, as well as on the final output [8]. Therefore, the process parameters of HME should be adjusted based on the physicochemical properties of each formulation component. Theoretically, the extrusion temperature should be set at 10–20 °C above the T_g of the polymer to facilitate the extrudability of materials during the extrusion process. In addition, there are many other properties that can be critical for HME, such as the polymer melt viscosity, molecular weight, and miscibility. Furthermore, the plasticization effect of the drug on the polymer may significantly affect the extrudability of materials [15]. Besides, many research studies have shown that P-CO_2 plasticizes some pharmaceutical polymers [30,31].

In this study, the extrusion temperature and drug/polymer ratio were found to have a major influence on the HME process. Extrusion of the pure polymer was impossible when the extrusion temperature was set below 160 °C because the maximum motor load was exceeded. At 160, 165, and 170 °C, the motor load approached the maximum. This could be attributed to a high melt viscosity of the polymer. To reduce the motor load, the screw speed of the extruder was reduced to 75 rpm at all studied temperatures (Table 3); however, the impact was very limited. Moreover, high torque values were observed, with P-CO_2 injection showing no plasticizing effect on HPMCAS LG. Therefore, it was not reasonable to inject P-CO_2 at such a high motor load. In fact, the extruder exhibited an increase in the motor load even with an increasing extruder temperature, which could be explained by the inability of the P-CO_2 stream to penetrate the polymer. Table 3 shows the results and conditions used for the investigation of the extruder parameters, i.e., the polymer/drug ratios in the HME processes with and without P-CO_2 injection. Injecting P-CO_2 at zones 4 and 6 provided relatively long periods of contact between the polymer and the injected P-CO_2 before the extruder die was reached. Additionally, at zones 4 and 6 (Fig. 1), the possibility of a back-pressure issue in the extruder was high, which spread the materials out of the feeding zone. Upon injection of P-CO_2 at zone 8 (Fig. 1), the formulation components and P-CO_2 were in contact only at zones 9 and 10. The injection of P-CO_2 at zone 8 was desirable to successfully produce foamy, porous extrudates (Fig. 1).

3.2. TGA analysis and drug content

The TGA data demonstrated that all formulations used in this study were stable at the employed processing temperature (data not shown). UV analysis showed acceptable drug content uniformity in the extrudates, indicating no loss of EFA as a function of the temperature and pressure during HME, with and without P-CO_2 injection. This confirmed that EFA was uniformly distributed in the formulations, with a high yield. The experimentally obtained drug contents corresponded to the theoretical values, ranging from 96% to 102%.

3.3. Differential scanning calorimetry

As shown in Fig. 2,, the DSC thermograms of pure EFA showed a characteristic endothermic peak at approximately 140 °C. The sharp EFA peak disappeared in all processed formulations but was retained in the respective physical mixtures, which showed smaller endothermic peaks (lower T_m), with a lower enthalpy of fusion. The absence of the peak indicated that all processed formulations had an amorphous nature after HME coupled with P-CO_2 processing.

3.4. Powder X-ray diffraction measurements

The diffraction patterns of pure EFA, pure HPMCAS LG, all processed formulations, and their respective physical mixtures are shown in Fig. 3. Analysis of the XRD pattern of the pure EFA sample showed characteristic peaks, indicating the crystalline nature of EFA. On the other hand, the diffraction pattern of pure HPMCAS LG did not show any peaks (hollow band), which indicated that its polymeric structure was amorphous. The XRD patterns of the physical mixtures of EFA and HPMCAS LG showed less intense peaks, owing to the partial presence of EFA in the crystalline form. Meanwhile, the EFA/HPMCAS LG extrudates did

not show these characteristic peaks, indicating the transformation of crystalline EFA into an amorphous form, which was consistent with the DSC data. Finally, comparison of the diffractograms of the processed formulations, obtained with and without P-CO_2 treatment, confirmed that the treatment caused no modifications.

3.5. Dissolution studies

HPMCAS LG enhanced the EFA dissolution rate in proportion to the HPMCAS LG content in the formulations. Fig. 4 shows the dissolution of EFA from various extrudates in the dissolution medium (pH 6.8). The order of improvement in the drug dissolution for the formulations processed by this coupled technology (HME/P-CO_2) was 30% EFA/70% HPMCAS LG > 40% EFA/60% HPMCAS LG > 50% EFA/50% HPMCAS LG. These results can be attributed to the dissolution medium, which was more suitable for the HPMCAS LG polymer, and to the presence of a high percentage of the polymer.

Although the 50% EFA extrudate was highly porous compared with the 30% EFA extrudate (Fig. 5), the dissolution was the highest for the 30% EFA extrudate, which confirmed a high solubility of the HPMCAS LG polymer in the dissolution medium. Furthermore, it was observed that the HPMCAS substitution level (L grade) played an important role in enhancing the dissolution rate of EFA, which was released at a faster rate than pure EFA did. The higher succinoyl content in the L-grade polymer results in an increased hydrophilicity and erodibility, thereby improving the release of EFA from extrudates with a higher HPMCAS LG content. The dissolution profiles demonstrated a relatively higher release of EFA from the CO_2-treated materials. These extrudates were all amorphous, indicating that the release could be controlled as a function of the carbon dioxide treatment [24]. The HPMCAS LG matrix controlled the dissolution rate of the extrudates. The HPMCAS LG polymer was eroded, and the EFA molecules were simultaneously dissolved, owing to their presence in an amorphous state. Thus, there was no need to overcome the crystalline lattice energy.

The dissolution rate depends on the surface area of the material exposed to dissolution media [32]. Although the foamed extrudates had an increased surface area, the unmilled foams showed a significantly slower dissolution than did regular, milled extrudates.

Moreover, although the porous matrix exhibited a high surface area, the P-CO_2-processed 50% EFA/50% HPMCAS LG formulation, with a lower density, higher porosity (Table 4), and a larger pore size (Fig. 5P–R), had almost the same dissolution profile as the 50% EFA/50%HPMCAS LG formulation without P-CO_2 treatment. This result was attributed to visually observed particles that were floating and accumulating on the surface of the media, making these particles inaccessible to the media.

In contrast, the P-CO_2-processed 30% and 40% EFA/HPMCAS LG formulations sank into the dissolution media, allowing the dissolution process to proceed faster through the fully accessible surfaces [33]. Since P-CO_2-treated extrudates are more hygroscopic [24], water penetrated faster into the matrix compared with its penetration into extrudates not treated with P-CO_2.

3.6. Scanning electron microscopy

The surface of all processed extrudates subjected to P-CO_2 treatment, which are shown in the SEM images in Fig. 5, was quite different from that of extrudates prepared without P-CO_2. The latter extrudates were smoother than were the foamed and porous extrudates treated with P-CO_2. The effective surface area was larger in the case of the foamed samples, where EFA particles were exposed to the dissolution media and exhibited an increased release [33]. The internal and external porous structures of the solid dispersions shown in Fig. 5 can alter the physicomechanical properties of such formulations.

On the other hand, as shown in Fig. 5, the porous matrix exhibited a mesh-like framework, indicating that P-CO_2 uniformly penetrated during the process through the HPMCAS LG matrix. Thus, these images suggested that a homogeneous or heterogeneous porosity behavior could occur, depending on the drug load (30% to 50%). Homogeneous pores were formed during processing of the 40% and 50% EFA dispersions with P-CO_2 treatment. In contrast, in the case of the 30% drug load, heterogeneous pores were formed during processing of the dispersion with P-CO_2 treatment. The highly porous nature of the extrudates may be attributed to the plasticizing effect of EFA, which led to less viscous matrices and facilitated the homogeneous penetration of P-CO_2 throughout the matrix during processing [33]. This could be visually confirmed in images of extrudates processed without P-CO_2, which showed smoother surfaces.

3.7. Density and porosity

As shown in Table 4, all density values decreased with P-CO_2 injection because of the formation of foamy and porous matrices. Furthermore, the porosity values were higher in samples prepared with P-CO_2 treatment. This resulted in a larger surface area, which led to improved dissolution profiles of high-HPMCAS LG content extrudates [22]. In addition, P-CO_2 treatment exhibited a high free surface energy, which aided in stabilizing the amorphous form of the drug [37–40].

3.8. Milling efficiency

The influence of P-CO_2 on the milling efficiency of extrudates was evaluated. The extrudates without P-CO_2 treatment were glassy, which made them very difficult to mill to obtain a suitable particle size distribution. Table 5 displays the results of this study, which confirmed that the amounts of particles with selected sizes (<600, 250, and 125 μm), obtained after milling P-CO_2-treated formulations, were higher than those of the corresponding formulations obtained without P-CO_2 treatment. Moreover, the torque of the milling instrument during processing of P-CO_2-treated formulations was less than that needed for the corresponding formulations obtained without P-CO_2 treatment. The enhancement in the milling efficiency was due to the morphological changes of extrudates into foam-like structures, which was the result of P-CO_2 injection.

3.9. Physical and chemical stability

For solid dispersion systems to be applicable commercially, stability issues have to be resolved [41]. During processing or storage, the amorphous state of a formulation may potentially transform to a crystalline state [42]. The impact of moisture on stability of

amorphous formulations during storage is also an important concern because it may increase the polymer mobility and promote drug crystallization.

The DSC thermograms of EFA (30%, 40%, and 50%) in the extrudates confirmed that none of the formulations, with and without P-CO_2 treatment, displayed any sign of recrystallization after storage for 6 months (Fig. 6A-C). The physical appearance of the formulations was examined during storage, and photographs were taken and compared. The photographs showed no signs of changes in the color, morphology, and physical state of the formulations, both with and without P-CO_2 injection, as shown in (Fig. 7A-C). Further, the drug release results revealed no significant changes in the release profiles after a long-term storage, for 6 months (Fig. 8A-C). The similarity factor values (f2) for the release profiles between fresh and 6-month-old samples were more than 50 for the EFA formulations (30%, 40%, and 50%). The drug content after storage of all formulations was in an acceptable range (97.0% and 106.0%), according to USP, as shown in Fig. 9. The drug content of EFA in the extrudates indicated that EFA was chemically stable, with no sign of degradation or weight loss after storage for 6 months.

In a recent study, it has been reported that a higher content of succinoyl substitution in HPMCAS polymers resulted in a strong affinity toward hydrophobic drug surfaces, leading to the inhibition of the crystal growth of an API [43]. HPMCAS LG has the highest succinoyl content and the lowest acetyl content compared with those in the other HPMCAS grades (MG and HG).

HPMCAS LG enhanced the physical stability of highly loaded amorphous EFA (30%, 40%, and 50%) in all formulations by increasing the Tg of the miscible mixture, which resulted in a reduction in molecular mobility during storage. Moreover, the miscibility between HPMCAS LG and EFA had a very significant impact on the stabilization of extrudates in the case of a high EFA load [44]. Further, the high viscosity of HPMCAS LG had a very desirable influence on the stability of EFA at a high load [45].

4. Conclusion

Highly loaded EFA extrudates were successfully processed in the presence of P-CO_2. However, there was no significant plasticizing effect of P-CO_2 on the HPMCAS LG polymer with EFA. The use of HPMCAS LG resulted in good release profiles for all EFA-loaded extrudates, with and without P-CO_2 injection. However, the EFA-loaded extrudates obtained with P-CO_2 injection exhibited a relatively higher drug release than did those obtained without P-CO_2. Morphological changes in extrudates, with the formation of a foam-like structure after P-CO_2 injection, resulted in an increased porosity and surface area. Thus, the milling efficiency of the extrudates improved. Stability studies demonstrated that EFA retained its amorphous form, indicating stability of the drug within extrudates. In summary, it was demonstrated that HPMCAS LG is a promising carrier for the production of physically and chemically stable ASD systems via the HME technology.

Acknowledgements

This work was supported by Ashland Speciality Ingredients. This project was also partially supported by Grant Number P20GM104932 from the National Institute of General Medical Sciences and the Biopharmaceutics-Clinical and Translational Core E of the COBRE, a component of the National Institutes of Health.

References

[1]. Crowley MM et al., “Pharmaceutical applications of hot-melt extrusion: Part I,” Drug Dev. Ind. Pharm., vol. 33, no. 9, pp. 909–926, 2007. [PubMed: 17891577]

[2]. Pimparade MB et al., “Development of taste masked caffeine citrate formulations utilizing hot melt extrusion technology and in vitro-in vivo evaluations,” Int. J. Pharm., vol. 487, no. 1–2, pp. 167–176, 2015. [PubMed: 25888797]

[3]. Morott JT et al., “The effects of screw configuration and polymeric carriers on hot-melt extruded taste-masked formulations incorporated into orally disintegrating tablets,” J. Pharm. Sci., vol. 104, no. 1, pp. 124–134, 2015. [PubMed: 25410968]

[4]. Maniruzzaman M, Rana MM, Boateng JS, Mitchell JC, and Douroumis D, “Dissolution enhancement of poorly water-soluble APIs processed by hot-melt extrusion using hydrophilic polymers,” Drug Dev. Ind. Pharm., vol. 39, no. 2, pp. 218–227, 2013. [PubMed: 22452601]

[5]. Repka MA, Majumdar S, Battu SK, Srirangam R, and Upadhye SB, “Applications of hot-melt extrusion for drug delivery,” Expert Opin. Drug Deliv., vol. 5, no. 12, pp. 1357–1376, 2008. [PubMed: 19040397]

[6]. Thomas S and Weimin Y, Advances in polymer processing. Woodhead Publishing Ltd, 2009.

[7]. LaFountaine JS, McGinity JW, and Williams RO, “Challenges and Strategies in Thermal Processing of Amorphous Solid Dispersions: A Review,” AAPS PharmSciTech, vol. 17, no. 1, pp. 43–55, 2016. [PubMed: 26307759]

[8]. Repka MA et al., “Melt extrusion: process to product,” Expert Opin. Drug Deliv., vol. 9, no. 1, pp. 105–125, Jan. 2012. [PubMed: 22145932]

[9]. Qian F, Huang J, and Hussain MA, “Drug–Polymer Solubility and Miscibility: Stability Consideration and Practical Challenges in Amorphous Solid Dispersion Development,” J. Pharm. Sci., vol. 99, no. 7, pp. 2941–2947, 2010. [PubMed: 20127825]

[10]. Marsac PJ, Shamblin SL, and Taylor LS, “Theoretical and practical approaches for prediction of drug-polymer miscibility and solubility,” Pharm. Res., vol. 23, no. 10, pp. 2417–2426, 2006. [PubMed: 16933098]

[11]. Kyerematen SO, Pudlas M, and Woehrle GH, “A fast and reliable empirical approach for estimating solubility of crystalline drugs in polymers for hot melt extrusion formulations,” J. Pharm. Sci., vol. 103, no. 9, pp. 2847–2858, 2014. [PubMed: 24634063]

[12]. Shah S, Maddineni S, Lu J, and Repka MA, “Melt extrusion with poorly soluble drugs,” Int. J. Pharm., vol. 453, no. 1, pp. 233–252, 2013. [PubMed: 23178213]

[13]. Gupta SS, Solanki N, and Serajuddin ATM, “Investigation of Thermal and Viscoelastic Properties of Polymers Relevant to Hot Melt Extrusion, IV: Affinisol™ HPMC HME Polymers,” AAPS PharmSciTech, vol. 17, no. 1, pp. 148–157, 2016. [PubMed: 26511936]

[14]. Kolter K, Karl M, and Gryczke A, Introduction to Solid Dispersions. 2012.

[15]. Chokshi RJ, Sandhu HK, Iyer RM, Shah NH, Malick AW, and Zia H, “Characterization of physico-mechanical properties of indomethacin and polymers to assess their suitability for hot-melt extrusion processs as a means to manufacture solid dispersion/solution,” J. Pharm. Sci., vol. 94, no. 11, pp. 2463–2474, 2005. [PubMed: 16200544]

[16]. Verreck G et al., “The effect of pressurized carbon dioxide as a temporary plasticizer and foaming agent on the hot stage extrusion process and extrudate properties of solid dispersions of itraconazole with PVP-VA 64,” Eur. J. Pharm. Sci., vol. 26, no. 3–4, pp. 349–358, 2005. [PubMed: 16137869]

[17]. Verreck G, “The Influence of Plasticizers in Hot-Melt Extrusion,” in Hot-Melt Extrusion: Pharmaceutical Applications, Chichester, UK: John Wiley & Sons, Ltd, 2012, pp. 93–112.

[18]. Wu C and McGinity JW, “Influence of methylparaben as a solid-state plasticizer on the physicochemical properties of Eudragit® RS PO hot-melt extrudates,” Eur. J. Pharm. Biopharm., vol. 56, no. 1, pp. 95–100, 2003. [PubMed: 12837487]

[19]. Repka MA, Gerding TG, Repka SL, and McGinity JW, “Influence of plasticizers and drugs on the physical-mechanical properties of hydroxypropylcellulose films prepared by hot melt extrusion,” Drug Dev. Ind. Pharm., vol. 25, no. 5, pp. 625–633, 1999. [PubMed: 10219532]

[20]. Mehuys E, Vervaet C, and Remon JP, “Hot-melt extruded ethylcellulose cylinders containing a HPMC-Gelucire® core for sustained drug delivery,” J. Control. Release, vol. 94, no. 2–3, pp. 273–280, 2004. [PubMed: 14744479]

[21]. Sauceau M, Fages J, Common A, Nikitine C, and Rodier E, “New challenges in polymer foaming: A review of extrusion processes assisted by supercritical carbon dioxide,” Prog. Polym. Sci., vol. 36, no. 6, pp. 749–766, 2011.

[22]. Ashour EA et al., “Influence of pressurized carbon dioxide on ketoprofen-incorporated hot-melt extruded low molecular weight hydroxypropylcellulose,” Drug Dev. Ind. Pharm., vol. 42, no. 1, pp. 123–130, 2016. [PubMed: 25997363]

[23]. Verreck G et al., “The effect of pressurized carbon dioxide as a plasticizer and foaming agent on the hot melt extrusion process and extrudate properties of pharmaceutical polymers,” J. Supercrit. Fluids, vol. 38, no. 3, pp. 383–391, 2006.

[24]. Verreck G et al., “The effect of supercritical CO2as a reversible plasticizer and foaming agent on the hot stage extrusion of itraconazole with EC 20 cps,” J. Supercrit. Fluids, vol. 40, no. 1, pp. 153–162, 2007.

[25]. Curatolo W, Nightingale JA, and Herbig SM, “Utility of hydroxypropylmethylcellulose acetate succinate (HPMCAS) for initiation and maintenance of drug supersaturation in the GI milieu,” Pharm. Res., vol. 26, no. 6, pp. 1419–1431, 2009. [PubMed: 19277850]

[26]. Ueda K, Higashi K, Yamamoto K, and Moribe K, “Inhibitory Effect of Hydroxypropyl Methylcellulose Acetate Succinate on Drug Recrystallization from a Supersaturated Solution Assessed Using Nuclear Magnetic Resonance Measurements,” Mol. Pharm., vol. 10, no. 10, pp. 3801–3811, 2013. [PubMed: 24025080]

[27]. Warashina S, Maruyama N, Quadir A, Obara S, editors, “Evaluation of a new development grade of hypromellose acetate succinate (HPMCAS) for solid dispersion by hot melt extrusion,” AAPS Annu. Meet., 2014.

[28]. Alshahrani SM, Lu W, Park J-B, Morott JT, Alsulays BB, Majumdar S, Langley N, Kolter K, Gryczke A, and Repka MA, "Stability-enhanced hot-melt extruded amorphous solid dispersions via combinations of Soluplus® and HPMCAS-HF," AAPS PharmSciTech. 2015 8;16(4):824–34. [PubMed: 25567525]

[29]. Joshi DC, Das SK, and Mukherjee RK, “Physical Properties of Pumpkin Seeds,” J. Agric. Eng. Res., vol. 54, no. 3, pp. 219–229, Mar. 1993.

[30]. Verreck G et al., “Hot stage extrusion of p-amino salicylic acid with EC using CO2as a temporary plasticizer,” Int. J. Pharm., vol. 327, no. 1–2, pp. 45–50, 2006. [PubMed: 16930886]

[31]. Lyons JG et al., “Preparation of monolithic matrices for oral drug delivery using a supercritical fluid assisted hot melt extrusion process,” Int. J. Pharm., vol. 329, no. 1–2, pp. 62–71, 2007. [PubMed: 17010544]

[32]. Verreck G, Six K, Van den Mooter G, Baert L, Peeters J, and Brewster ME, “Characterization of solid dispersions of itraconazole and hydroxypropylmethylcellulose prepared by melt extrusion—part I,” Int. J. Pharm., vol. 251, no. 1–2, pp. 165–174, 2003. [PubMed: 12527186]

[33]. Nagy ZK et al., “Use of supercritical CO2-aided and conventional melt extrusion for enhancing the dissolution rate of an active pharmaceutical ingredient,” Polym. Adv. Technol., vol. 23, no. 5, pp. 909–918, 2012.

[34]. Almutairy BK et al., “Development of Floating Drug Delivery System with Superior Buoyancy in Gastric Fluid using Hot-Melt Extrusion Coupled with Pressurized CO2,” Pharmazie, vol. 71, pp. 1–6, 2015.

[35]. Lee M, Tzoganakis C, and Park CB, “Extrusion of PE/PS blends with supercritical carbon dioxide,” Polym. Eng. Sci., vol. 38, no. 7, pp. 1112–1120, 1998.

[36]. Park CB, Baldwin DF, and Suh NP, “Effect of the pressure drop rate on cell nucleation in continuous processing of microcellular polymers,” Polym. Eng. Sci., vol. 35, no. 5, pp. 432–440, 1995.

[37]. Laitinen R, Löbmann K, Strachan CJ, Grohganz H, and Rades T, “Emerging trends in the stabilization of amorphous drugs,” Int. J. Pharm., vol. 453, no. 1, pp. 65–79, 2013. [PubMed: 22569230]

[38]. Jackson CL and McKenna GB, “Vitrification and Crystallization of Organic Liquids Confined to Nanoscale Pores,” Chem. Mater., vol. 8, no. 8, pp. 2128–2137, 1996.

[39]. Prestidge CA, Barnes TJ, Lau C-H, Barnett C, Loni A, and Canham L, “Mesoporous silicon: a platform for the delivery of therapeutics,” Expert Opin. Drug Deliv., vol. 4, no. 2, pp. 101–110, 2007. [PubMed: 17335408]

[40]. Qian KK and Bogner RH, “Application of Mesoporous Silicon Dioxide and Silicate in Oral Amorphous Drug Delivery Systems,” J. Pharm. Sci., vol. 101, no. 2, pp. 444–463, 2012. [PubMed: 21976048]

[41]. Vasconcelos T, Sarmento B, and Costa P, “Solid dispersions as strategy to improve oral bioavailability of poor water soluble drugs,” Drug Discov. Today, vol. 12, no. 23–24, pp. 1068–1075, Dec. 2007. [PubMed: 18061887]

[42]. Johari GP, Kim S, and Shanker RM, “Dielectric studies of molecular motions in amorphous solid and ultraviscous acetaminophen,” J. Pharm. Sci., vol. 94, no. 10, pp. 2207–2223.

[43]. Ueda K, Higashi K, Yamamoto K, and Moribe K, “Inhibitory Effect of Hydroxypropyl Methylcellulose Acetate Succinate on Drug Recrystallization from a Supersaturated Solution Assessed Using Nuclear Magnetic Resonance Measurements,”Mol. Pharm., vol.10, no. 10, pp. 3801–3811, 2013. [PubMed: 24025080]

[44]. Marsac PJ, Rumondor ACF, Nivens DE, Kestur US, Stanciu Lia., and Taylor LS, “Effect of temperature and moisture on the miscibility of amorphous dispersions of felodipine and poly(vinyl pyrrolidone),” J. Pharm. Sci., vol. 99, no. 1, pp. 169–185, 2010. [PubMed: 19492305]

[45]. Chokshi R and Zia H, “Hot-Melt Extrusion Technique: A Review,” Iran. J. Pharm. Res., vol. Volume 3, no. Number 1, pp. 3–16, 2010.

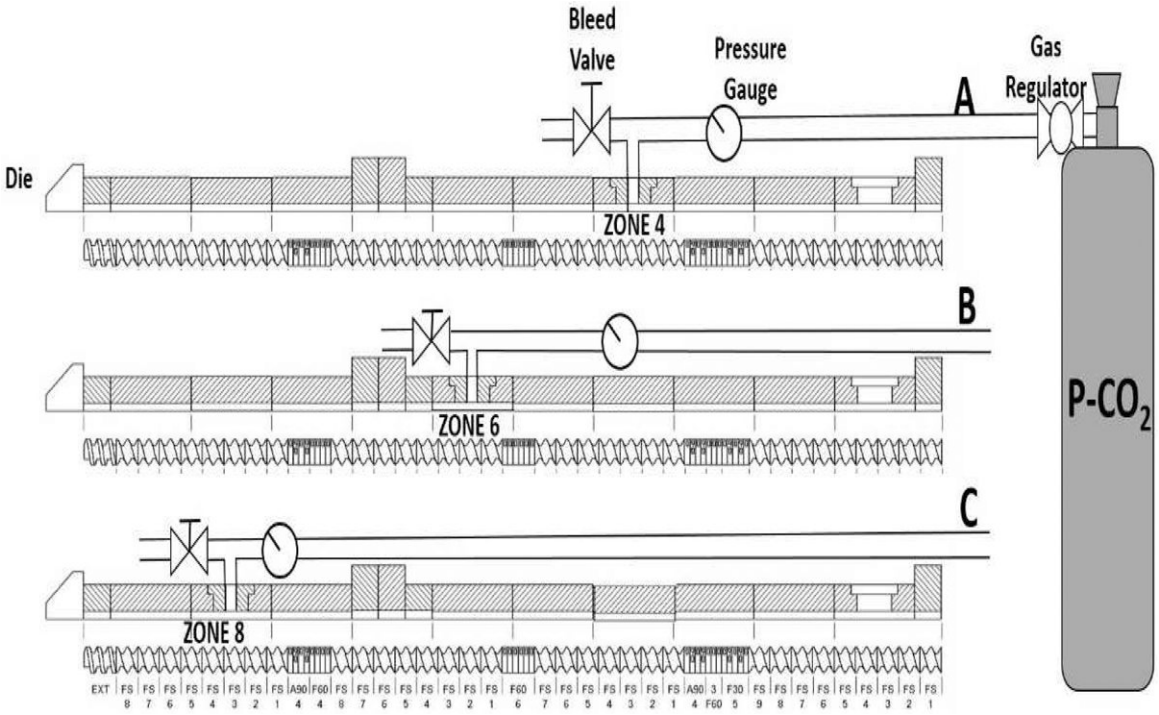

Figure 1.

Schematic representation for the set-up of the combined HME/P-CO_2 techniques; Injection of P-CO_2 at (A) Zone 4; (B) Zone 6; (C) Zone 8

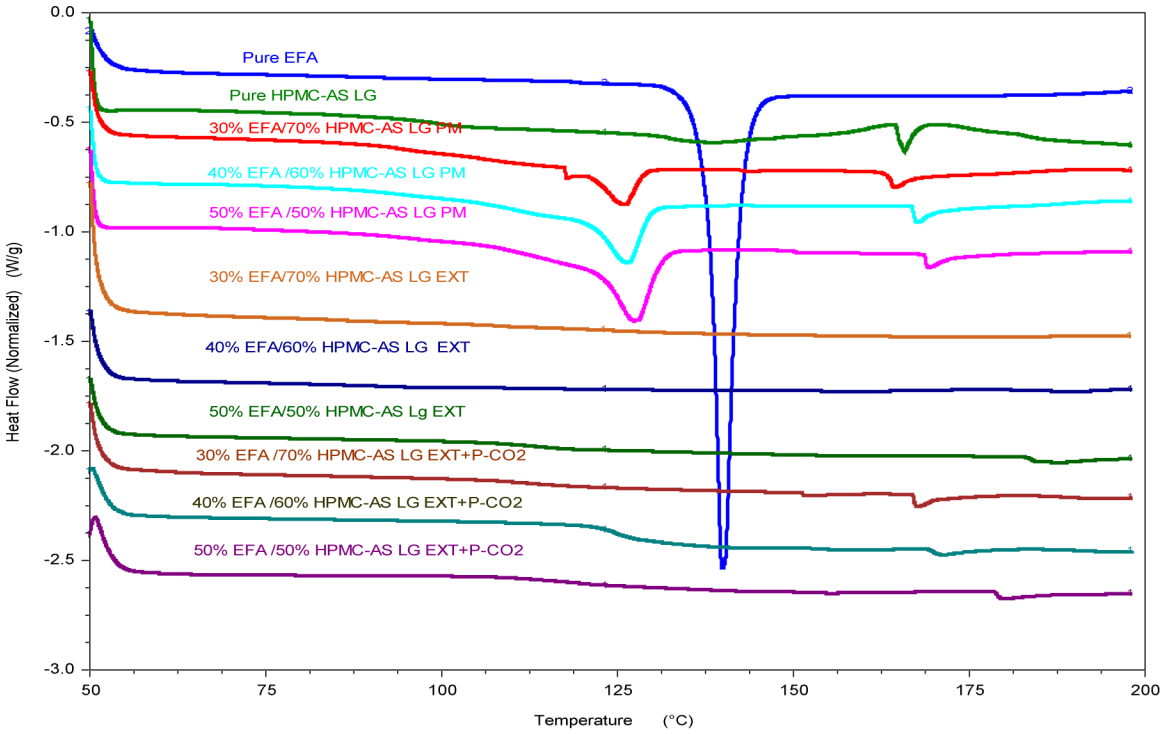

Figure 2.

DSC thermograms of pure EFA, pure HPMC-AS LG, physical mixtures (PM) and extrudates (EXTs) with and without P-CO_2

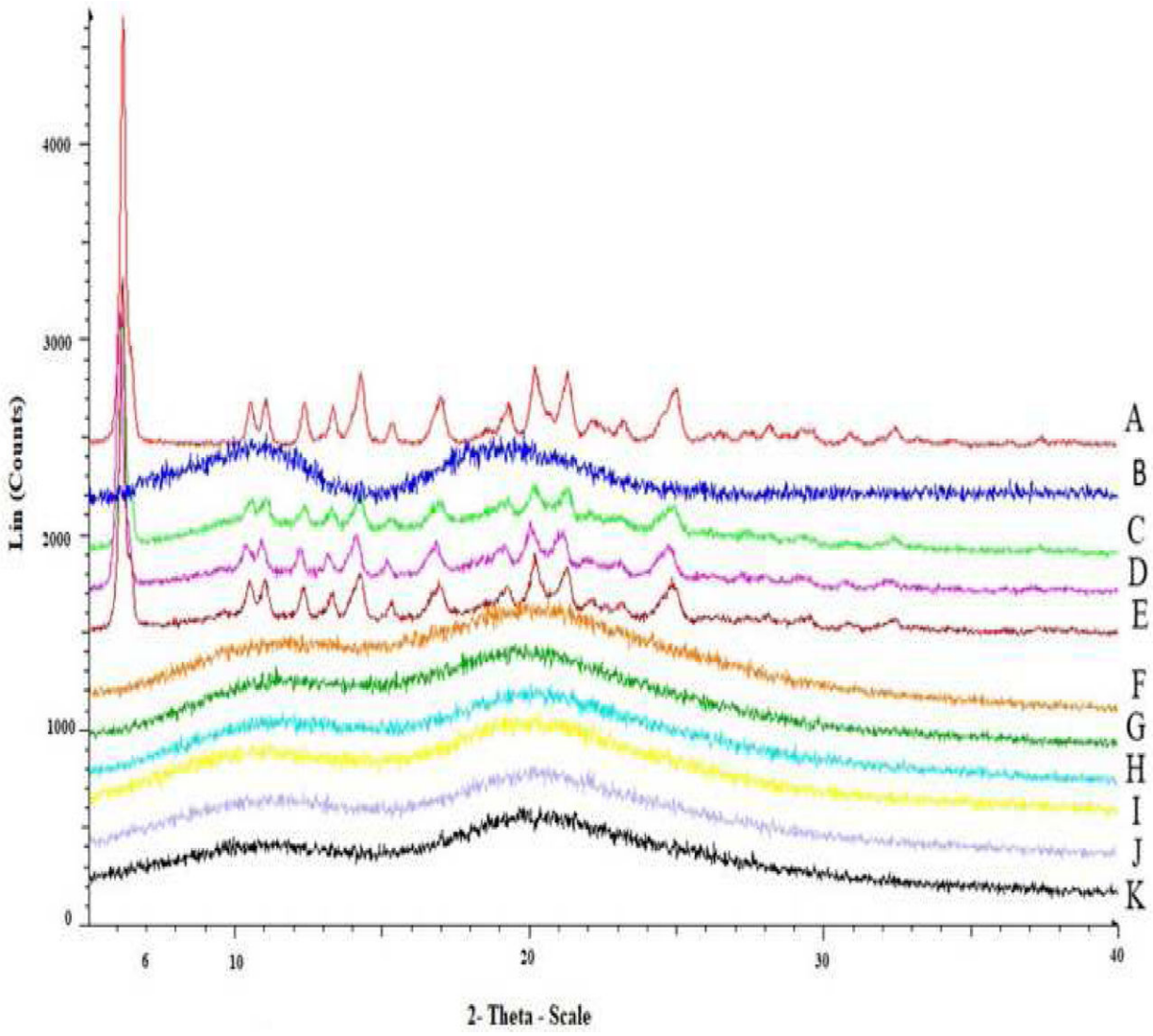

Figure 3.

(A): PXRD diffractograms of pure crystalline EFA, (B): PXRD diffractograms of pure HPMC-AS LG; (C, D, and E): PXRD diffractograms of %30, %40, and %50 EFA/ HPMC-AS LG PM; (F, G, and H): PXRD diffractograms of %30, %40, and %50 EFA/ HPMC-AS LG without P-CO_2; (I, J, and K): PXRD diffractograms of %30, %40, and %50 EFA/ HPMC-AS LG with P-CO_2

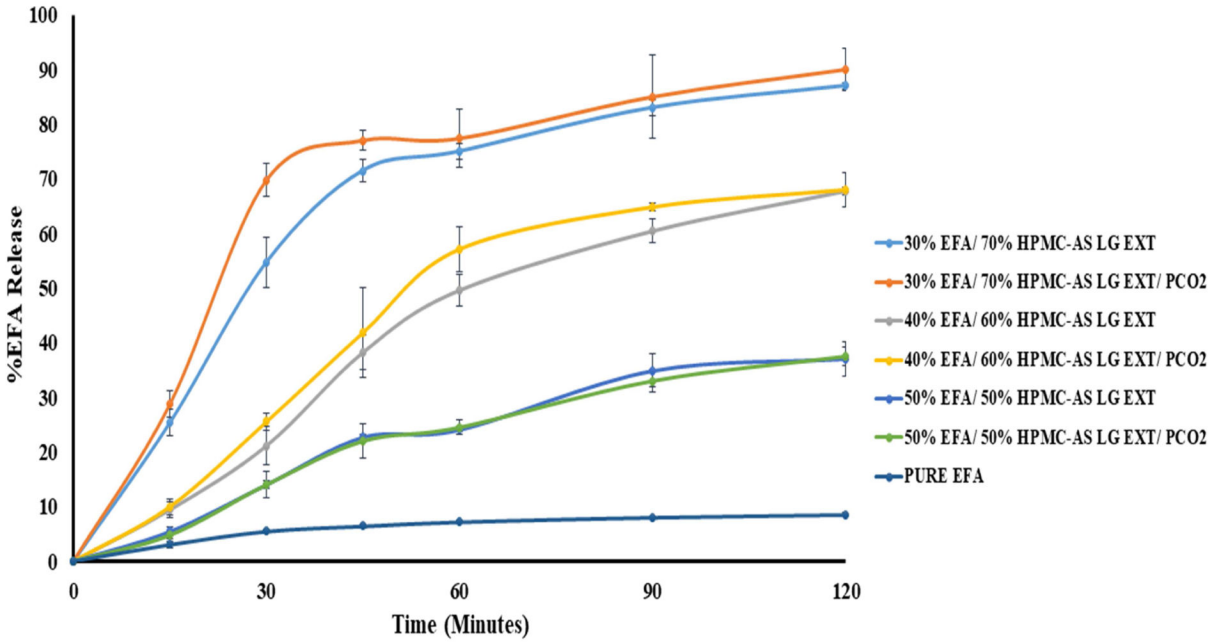

Figure 4.

In-Vitro release profiles of extrudates with and without P-CO_2 (A USP dissolution apparatus II, 50 rpm, pH 6.8 phosphate buffer at 37 ± 0.5 °C for 2 h)

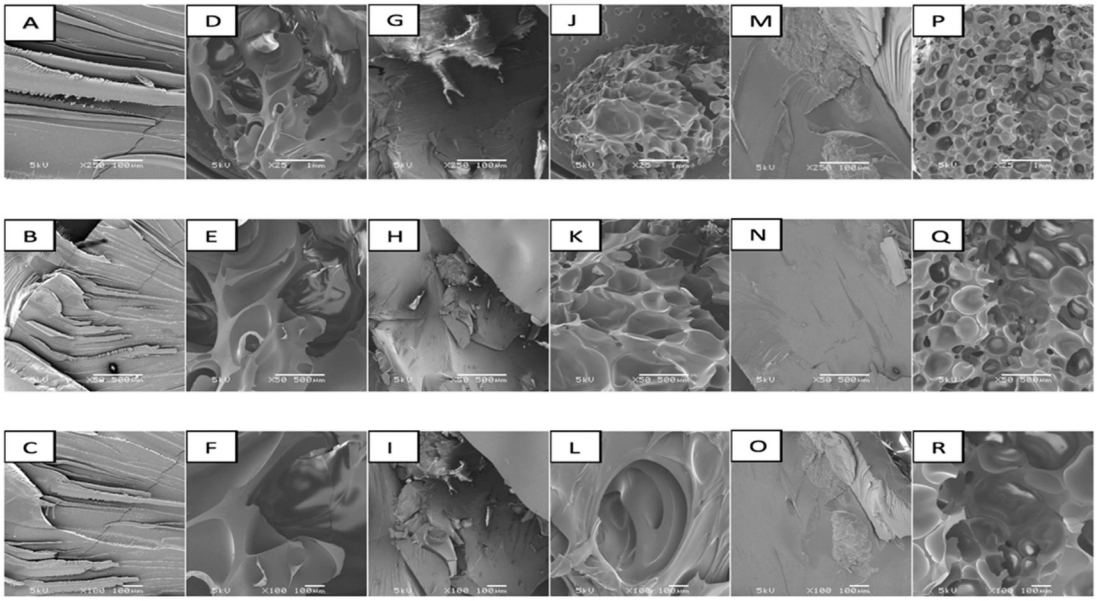

Figure 5.

SEM images of HPMC-AS LG Extrudates with and without P-CO_2; A, B, and C: 30 % Extrudate (30% EFA / 70% HPMC-AS LG without P-CO_2) D, E, and F: 30 % Extrudate (30% EFA / 70% HPMC-AS LG with P-CO_2) G, H, and I: 40 % Extrudate (40% EFA / 60% HPMC-AS LG without P-CO_2) J, K, and L: 40 % Extrudate (40% EFA / 60% HPMC-AS LG with P-CO_2) M, N, and O: 50 % Extrudate (50% EFA / 50% HPMC-AS LG without P-CO_2) P, Q, and R: 50 % Extrudate (50% EFA / 50% HPMC-AS LG with P-CO_2)

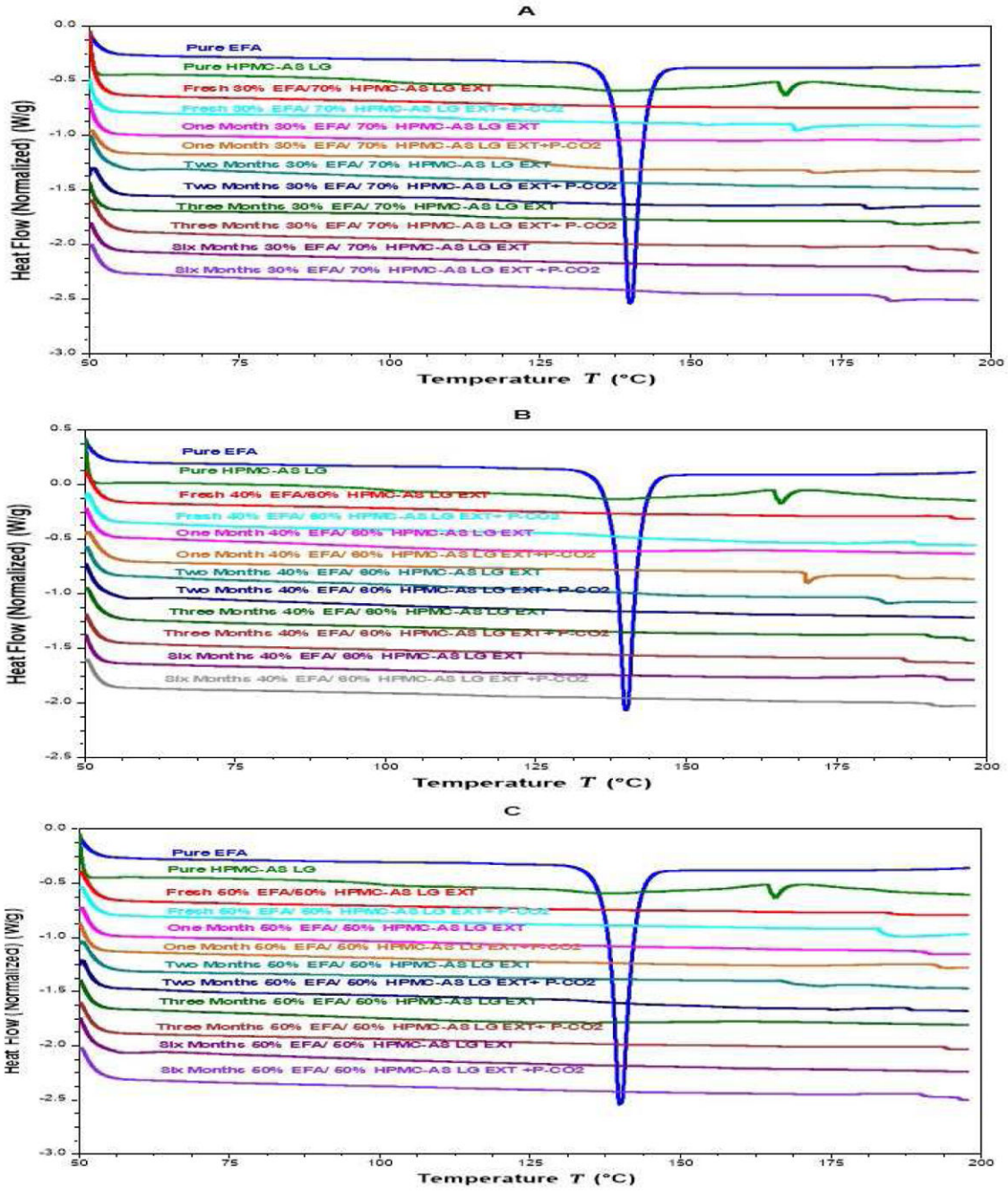

Figure 6.

DSC thermograms of extrudates with and without P-CO_2 Stored at 25°C/60% RH. (A): formulations 30 % Extrudate (30% EFA / 70% HPMC-AS LG); (B): formulations 40 % Extrudate (40% EFA / 60% HPMC-AS LG); and (C): formulations 50 % Extrudate (50% EFA / 50% HPMC-AS LG)

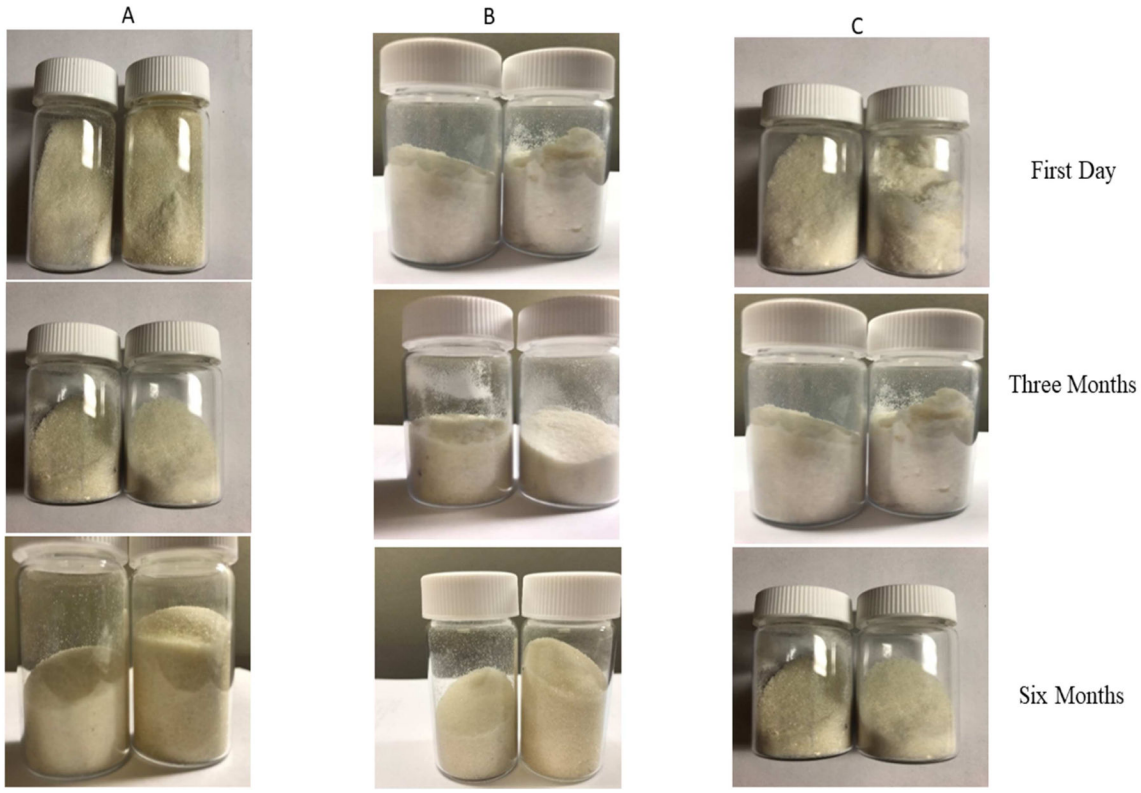

Figure 7.

Physical appearance of extrudates with and without P-CO_2 Stored at 25°C/60% RH. (A): formulation 30 % Extrudate (30% EFA / 70% HPMC-AS LG), (B): formulations 40 % Extrudate (40% EFA / 60% HPMC-AS LG), and (C): formulations 50 % Extrudate (50% EFA / 50% HPMC-AS LG)

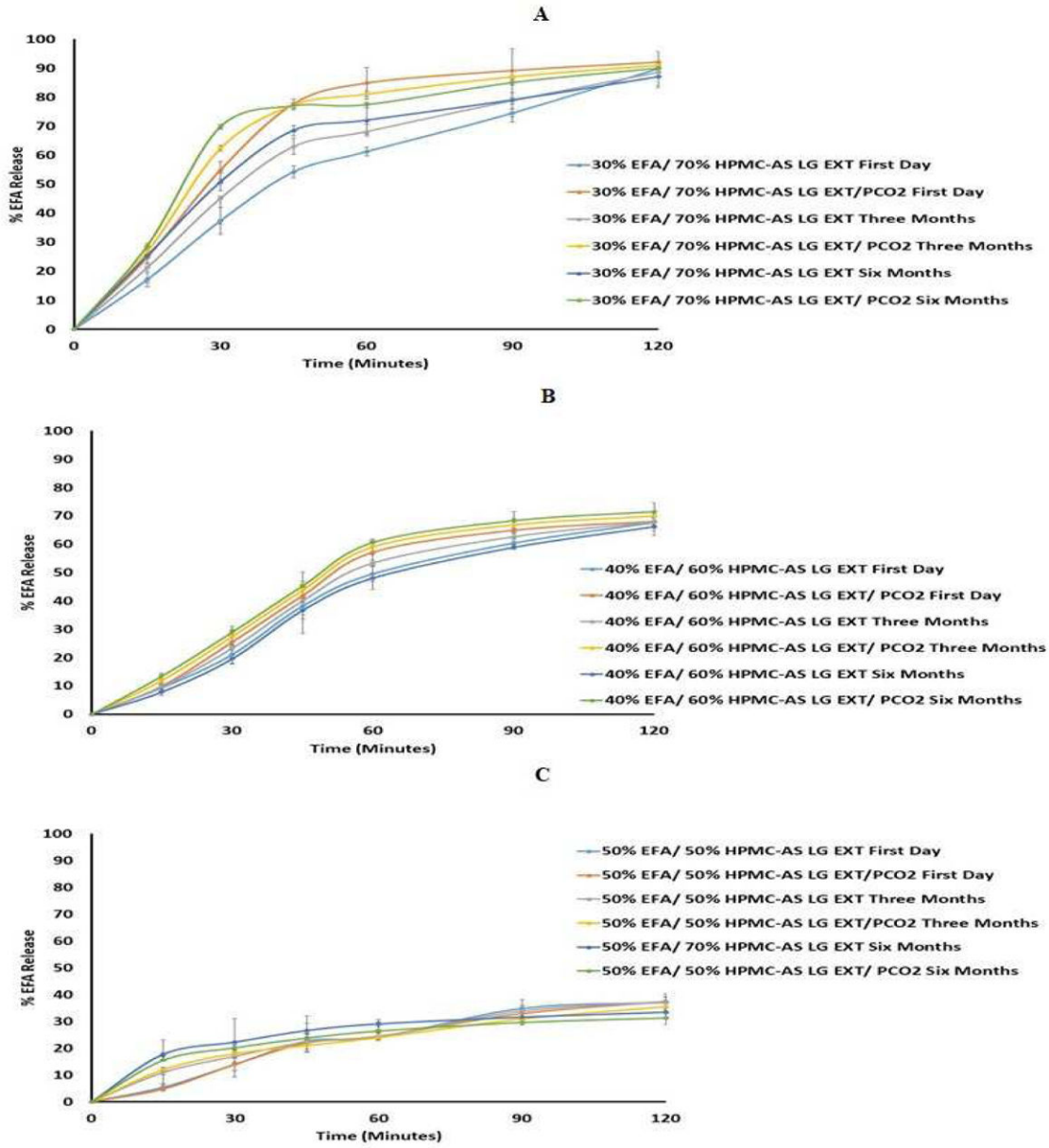

Figure 8.

In-Vitro release profile of extrudates with and without P-CO_2 (A USP dissolution apparatus II, 50 rpm, pH 6.8 phosphate buffer at 37 ± 0.5 °C for 2 h) stored at 25°C/60% RH. (A): formulation 30 % Extrudate (30% EFA / 70% HPMC-AS LG), (B): formulation 40 % Extrudate (40% EFA / 60% HPMC-AS LG), and (C): formulation 50 % Extrudate (50% EFA / 50% HPMC-AS LG)

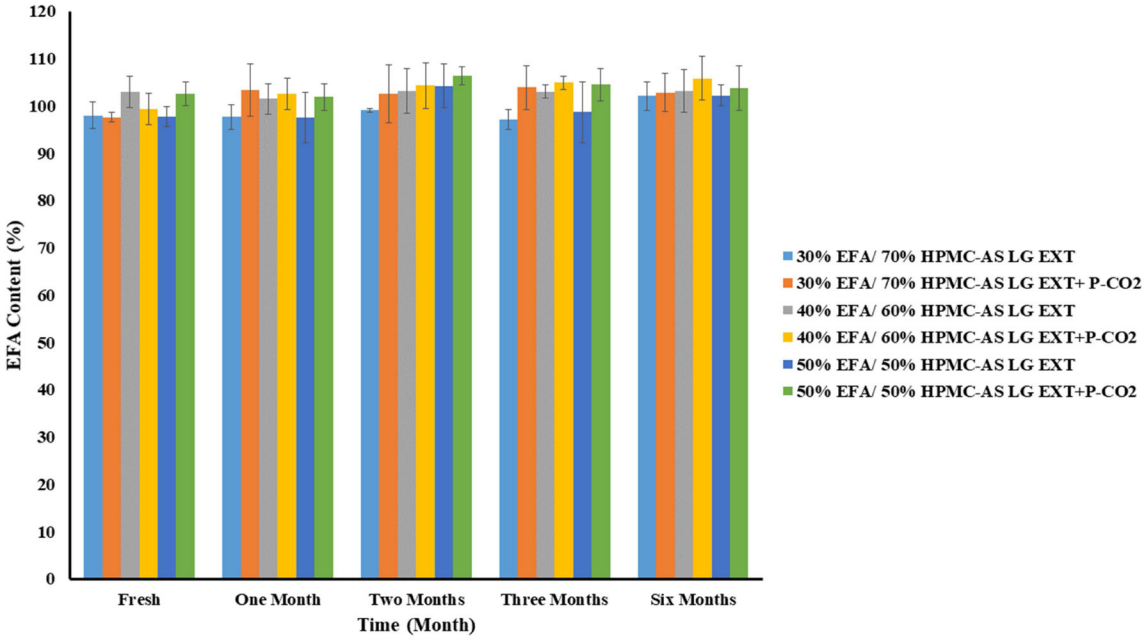

Figure 9.

Drug contents of EFA extrudates with and without P-CO_2 Stored at 25°C/60% RH

Table 1.

The preliminary processing trials of HPMC-AS LG polymer by hot-melt extrusion

Formulations	Processing Temperature (°C)	Screw Speed (rpm)	Barrel Torque (%)
100% HPMC-AS LG	140	100	Maximum
100% HPMC-AS LG	140	75	Maximum
100% HPMC-AS LG	140	100	Maximum
100% HPMC-AS LG	140	75	Maximum
100% HPMC-AS LG	150	100	Maximum
100% HPMC-AS LG	150	75	Maximum
100% HPMC-AS LG	150	100	Maximum
100% HPMC-AS LG	150	75	Maximum
100% HPMC-AS LG	160	100	98
100% HPMC-AS LG	160	75	88
100% HPMC-AS LG	170	100	88-90
100% HPMC-AS LG	170	75	82
100% HPMC-AS LG	190	100	84-92
100% HPMC-AS LG	190	75	80-90
100% HPMC-AS LG	190	100	84-92
100% HPMC-AS LG	190	75	80-90

J Drug Deliv Sci Technol. Author manuscript; available in PMC 2020 August 01.

Table 2.

Conditions and outcomes for optimized formulations during HME processes

Formulations	Processing Temperature (°C)	Screw Speed (rpm)	Barrel Torque (%)	P-CO_2 (PSI)	P-CO_2 Injection Zone
30% EFA/ 70% HPMC-AS LG EXT	140	100	46	300-400	Zone 8
30% EFA/ 70% HPMC-AS LG EXT	140	100	46	-	-
40% EFA/ 60% HPMC-AS LG EXT	140	100	33	300-400	Zone 8
40% EFA/ 60% HPMC-AS LG EXT	140	100	33	-	-
50% EFA/ 50% HPMC-AS LG EXT	140	100	27	300-400	Zone 8
50% EFA/ 50% HPMC-AS LG EXT	140	100	27	-	-
30% EFA/ 70% HPMC-AS LG EXT*	150	75	25-30	250-300	Zone 8
30% EFA/ 70% HPMC-AS LG EXT*	150	75	25-30	-	-
40% EFA/ 60% HPMC-AS LG EXT*	150	75	20-25	250-300	Zone 8
40% EFA/ 60% HPMC-AS LG EXT*	150	75	20-25	-	-
50% EFA/ 50% HPMC-AS LG EXT*	150	75	13-20	250-300	Zone 8
50% EFA/ 50% HPMC-AS LG EXT*	150	75	13-20	-	-

*These formulations were selected for further studies.

Table 3.

Extrusion conditions and parameters of various polymer/ drug ratio compositions with and without P-CO_2 injection

Formulations	Processing Temperature (°C)	Screw Speed (rpm)	Barrel Torque (%)	P-CO_2 Injection Zone 4	P-CO_2 Injection Zone 6	P-CO_2 Injection Zone 8	P-CO_2 (PSI)	Back Pressure	Feeding Zone Blockage	HME Process
100% HPMC-AS LG	140	100	Maximum *	-	-	-	-	-	-	Failed
100% HPMC-AS LG	140	75	Maximum	-	-	-	-	-	-	Failed
100% HPMC-AS LG	140	100	Maximum	√	√	-	-	High	-	Failed
100% HPMC-AS LG	140	75	Maximum	√	√	-	-	High	-	Failed
100% HPMC-AS LG	150	100	Maximum	-	-	-	-	-	-	Failed
100% HPMC-AS LG	150	75	Maximum	-	-	-	-	-	-	Failed
100% HPMC-AS LG	150	100	Maximum	√	√	-	-	High	-	Failed
100% HPMC-AS LG	150	75	Maximum	√	√	-	-	High	-	Failed
100% HPMC-AS LG	160	100	$98^{H.TQ}$	√	√	-	-	High	-	Successful **
100% HPMC-AS LG	160	75	$88^{H.TQ}$	√	√	-	-	High	-	Successful **
100% HPMC-AS LG	170	100	$88\text{-}90^{H.TQ}$	√	√	-	-	High	-	Successful **
100% HPMC-AS LG	170	75	$82^{H.TQ}$	√	√	-	-	High	-	Successful **
100% HPMC-AS LG	$190^{H.T}$	100	$84\text{-}92^{H.TQ}$	√	√	-	-	High	-	Successful **
100% HPMC-AS LG	$190^{H.T}$	75	$80\text{-}90^{H.TQ}$	√	√	-	-	High	-	Successful **
100% HPMC-AS LG	$190^{H.T}$	100	$84\text{-}92^{H.TQ}$	-	-	√	300-400	Low	No	Successful **
100% HPMC-AS LG	$190^{H.T}$	75	$80\text{-}90^{H.TQ}$	-	-	√	300-400	Low	No	Successful **
80% HPMC-AS LG/% 20 EFA	140	100	54	-	-	-	-	-	-	Successful
70% HPMC-AS LG/% 30 EFA	140	100	46	-	-	-	-	-	-	Successful
60% HPMC-AS LG/% 40 EFA	140	100	33	-	-	-	-	-	-	Successful
50% HPMC-AS LG/% 50 EFA	140	100	27	-	-	-	-	-	-	Successful
80% HPMC-AS LG/% 20 EFA	150	75	44	-	-	-	-	-	-	Successful
70% HPMC-AS LG/% 30 EFA	150	75	25-30	-	-	-	-	-	-	Successful
60% HPMC-AS LG/% 40 EFA	150	75	20-25	-	-	-	-	-	-	Successful
50% HPMC-AS LG/% 50 EFA	150	75	13-20	-	-	-	-	-	-	Successful

Formulations	Processing Temperature (°C)	Screw Speed (rpm)	Barrel Torque (%)	P-CO_2 Injection Zone 4	6	8	P-CO_2 (PSI)	Back Pressure	Feeding Zone Blockage	HME Process
80% HPMC-AS LG/% 20 EFA	140	100	54	-	-	√	300-400	Low	No	Successful
70% HPMC-AS LG/% 30 EFA	140	100	46	-	-	√	300-400	Low	No	Successful
60% HPMC-AS LG/% 40 EFA	140	100	33	-	-	√	300-400	Low	No	Successful
50% HPMC-AS LG/% 50 EFA	140	100	27	-	-	√	300-400	Low	No	Successful
80% HPMC-AS LG/% 20 EFA	150	75	44	-	-	√	250-350	Low	No	Successful
70% HPMC-AS LG/% 30 EFA	150	75	25-30	-	-	√	250-350	Low	No	Successful
60% HPMC-AS LG/% 40 EFA	150	75	20-25	-	-	√	250-350	Low	No	Successful
50% HPMC-AS LG/% 50 EFA	150	75	13-20	-	-	√	250-350	Low	No	Successful

*The motor load reached the maximum level in which it was impossible to move on.

**Very limited success to obtain the final product, but with very high motor load and high temperature.

H.T: Very high temperature.

H.TQ: Very high motor load (High Torque).

Table 4.

Bulk, tapped, true density and porosity of pure EFA, pure HPMC-AS LG, Physical Mixture (PM) and Extrudates (EXT) with and without P-CO_2 (g/ml)

Formulations	Bulk Density	Tapped Density	True Density	%Porosity
EFA	0.225	0.338	1.450	84.482
HPMC-AS LG	0.462	0.470	1.289	64.158
30% EFA / HPMC-AS LG PM	0.369	0.447	1.416	73.940
40% EFA / HPMC-AS LG PM	0.351	0.421	1.474	76.187
50% EFA / HPMC-AS LG PM	0.317	0.404	1.532	79.308
30% EFA / HPMC-AS LG EXT	0.598	0.629	1.347	55.605
40% EFA / HPMC-AS LG EXT	0.612	0.668	1.362	55.066
50% EFA / HPMC-AS LG EXT	0.620	0.652	1.381	55.104
30% EFA / HPMC-AS LG EXT+P-CO_2	0.494	0.493	1.350	63.407
40% EFA / HPMC-AS LG EXT+P-CO_2	0.461	0.519	1.357	66.028
50% EFA / HPMC-AS LG EXT+P-CO_2	0.350	0.466	1.382	74.674

J Drug Deliv Sci Technol. Author manuscript; available in PMC 2020 August 01.

Table 5.

Results of the Milling Efficiency

Formulations	Torque (Amps)	Particles < 600 um (%)	Particles < 250 um (%)	Particles < 125 um (%)
30% EFA / HPMC-AS LG EXT	1.08	78.44	9.57	1.03
40% EFA / HPMC-AS LG EXT	0.85	84.99	15.33	2.74
50% EFA / HPMC-AS LG EXT	0.79	77.90	3.37	0.98
30% EFA / HPMC-AS LG EXT P-CO_2	0.79	92.14	14.88	1.97
40% EFA / HPMC-AS LG EXT P-CO_2	0.74	97.70	24.41	4.75
50% EFA / HPMC-AS LG EXT P-CO_2	0.72	98.08	13.64	1.79